Quantum-phase and information-entropy dynamics of dimers interacting with a single-mode coherent field: The difference between one- and two-exciton models

ARTICLE *in* INTERNATIONAL JOURNAL OF QUANTUM CHEMISTRY · SEPTEMBER 2001

Impact Factor: 1.43 · DOI: 10.1002/qua.1407

2 AUTHORS, INCLUDING:

Masayoshi Nakano
Osaka University
337 PUBLICATIONS **4,781** CITATIONS

Quantum-Phase and Information-Entropy Dynamics of Dimers Interacting with a Single-Mode Coherent Field: The Difference between One- and Two-Exciton Models

M. NAKANO, K. YAMAGUCHI

Department of Chemistry, Graduate School of Science, Osaka University, Osaka, 560-0043, Japan

Received 6 June 2000; revised 6 February 2001; accepted 12 March 2001

ABSTRACT: We develop a numerically exact approach to the quantum-phase and information-entropy dynamics of a molecular aggregate interacting with quantized fields. It is well known that a peculiar quantum nature, i.e., collapses and revivals, is observed in monomer and noninteracting aggregate models. In this article, we investigate the intermolecular interaction effects on the collapse-revival behavior using several dimer models (composed of two-state monomers with different intermolecular distances) interacting with a single-mode coherent photon field. The intermolecular interaction is taken into account by using the dipole-dipole interaction. Also, one- and two-exciton dimer models are considered in order to elucidate the exciton contributions to collapse-revival behavior. This quantum behavior is analyzed from the viewpoint of the dynamics of Pegg–Barnett photon-phase and information-entropy of dimers, which closely relate to the time evolution of quantum coherency between the ground and the excited dimer states and the degree of the entanglement between dimer and photon, respectively. It is found that the intermolecular interaction and the two-exciton generation provide remarkable changes in the collapse-revival behavior through their significant influence on the quantum-phase dynamics and the photon-dimer entanglement. From the dimer entropy dynamics, intermediate intermolecular interaction is found to cause the momentary decrease in the photon-dimer correlation in the early time region. This feature leads to the enhancement of off-diagonal density (quantum coherency) between two dimers. Int J Quantum Chem 84: 530–545, 2001

Key words: quantum-phase; entropy; exciton; collapse-revival

Correspondence to: M. Nakano; e-mail: mnaka@chem.sci.osaka-u.ac.jp.

Contract grant sponsor: Ministry of Education, Science, Sports, and Culture of Japan.

Contract grant numbers: 10185101, 12042248, 12740320.

Introduction

The Jaynes–Cummings (JC) model [1], including two-state atom systems interacting with quantized photon fields, has been attracting interest due to its simplicity of treatment and its complex behavior in fully quantum nature. Various more complicated cases have been investigated theoretically [2–5], and some experimental realizations have also been achieved [6–8]. It is well known that the time evolution of the JC model exhibits repeated collapses and revivals of Rabi oscillations of atomic populations [1–11]. In general, in order to understand the dynamics of matter-photon field systems, the matter population, the average photon number, and the entropy of subsystems [12] are investigated. In addition to these quantities, quantum-phase properties of an external photon field have received much attention recently, especially after Pegg and Barnett introduced a Hermitian phase operator [13–15]. Using this phase operator, some JC models have been investigated [16–24]. As a computational approach to the study on such dynamics, we have developed a numerically exact calculation method, which is referred to as electron-photon field dynamics (EPFD) [18].

So far, the matter systems are mostly composed of single atom/molecule or noninteracting identical monomers. Recently, a few studies on a molecular aggregate involving the intermolecular interactions have been performed, and the dipole-dipole interaction is found to significantly affect the features of collapse-revival behavior [25, 26]. However, the photon-phase and information-entropy dynamics of such systems have not been revealed yet. Therefore, we performed a quantum dynamics (in two-exciton model) of *H*-aggregate-type dimers composed of two identical two-state monomers interacting with a single-mode coherent field [24]. First, the time evolution of photon-phase properties obtained by using the Pegg–Barnett (PB) phase operator [13–15] and that of the information entropy of dimer (which represents the degree of correlation between dimer and photon) are investigated in connection with the effects of intermolecular interaction on the collapse-revival behavior. We next elucidate the contributions of exciton states on the features of quantum dynamics by considering the one- and two-exciton dimer models. Finally, we discuss the effects of the intermolecular interaction and the considered exciton states on the photon-phase and molecular-entropy dynamics, as well as a prediction of the collapse-revival behavior of aggregate systems involving larger number of monomers interacting with a quantized field.

Methodology

CONSTRUCTION OF A STATE MODEL FOR A MOLECULAR AGGREGATE

In our calculation approach, we first construct a state model for a molecular aggregate and then perform the time evolution of the aggregate state model interacting with a quantized field. The monomer is approximated to be a dipole. This approximation is considered to be acceptable if the intermolecular distance (R) is larger than the size of a monomer. The kth monomer possesses a transition energy, E_{21}^k ($\equiv E_2^k - E_1^k = 37800\ \mathrm{cm}^{-1}$), and a transition moment, μ_{12} (=5 D) (see Figure 1). For two dipoles k and l, the angle between a dipole $k(l)$ and a line drawn from the dipole site k to l is $\theta_{k_l}(\theta_{l_k})$ (=90° for arbitrary k_l in the present case). A general form of Hamiltonian for arbitrary aggregate model composed of N'-state monomers ($N' \geq 2$, integer) is presented by

$$H_{\mathrm{agg}} = H_0 + V_{\mathrm{int}} = \sum_{k}^{N} \sum_{i_k}^{N'} E_{i_k}^k a_{i_k}^+ a_{i_k}$$

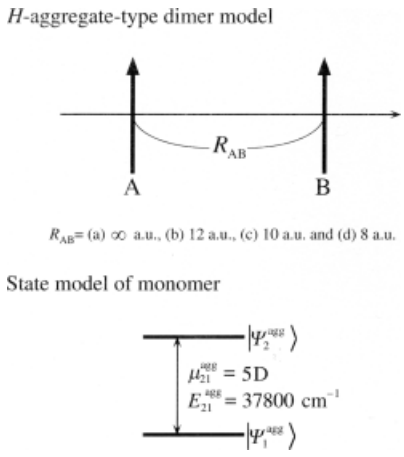

FIGURE 1. *H*-aggregate-type molecular dimers with several intermolecular distances (R): (a) $R = \infty$ a.u., (b) $R = 12$ a.u., (c) $R = 10$ a.u., (d) $R = 8$ a.u. The arrow represents a transition dipole of a monomer (a) two-state molecular model with transition energy $E_{21} (\equiv E_2 - E_1 = 37800\ \mathrm{cm}^{-1}$ and transition moment $\mu_{12} = 5$ D).

$$+\frac{1}{4\pi\varepsilon_0}\sum_{k<l}^{N}\sum_{\substack{i_k,i'_k\\ i_l,i'_l}}\mu^k_{i_k i'_k}\mu^l_{i_l i'_l}\left[\left(\cos(\theta_{k_l}-\theta_{l_k})-3\cos\theta_{k_l}\cos\theta_{l_k}\right)/R^3_{kl}\right]a^+_{i_k}a_{i'_k}a^+_{i_l}a_{i'_l}, \quad (1)$$

where the first (H_0) and the second represent a noninteracting Hamiltonian and the dipole–dipole interaction. $E^k_{i_k}$ is an energy of the state i_k for monomer k, and $\mu^k_{i_k i'_k}$ is a magnitude of a transition matrix element between states i_k and i'_k for monomer k. The $a^+_{i_k}$ and $a_{i'_k}$ represent, respectively, the creation and annihilation operators for the i_k state of monomer k. By using the basis for the aggregate $\{|\varphi^1_{i_1}\varphi^2_{i_2}\cdots\phi^N_{i_N}\rangle\}$, ($N$ is the number of monomers) which is constructed by a direct product of a state vector for each monomer $\{|\varphi^k_{i_k}\rangle\}$, the matrix elements of the second terms in Eq. (1) are presented in our previous paper [24].

By diagonalizing the Hamiltonian matrix H [Eq. (1)], we can obtain eigenenergies $\{E^{\mathrm{agg}}_l\}$ and eigenstates $\{|\psi^{\mathrm{agg}}_l\rangle\}$ ($l = 1,\ldots,M$), where M is the size of the basis used. The M is $1 + {}_NC_1 + {}_NC_2$ since we consider one and two excitons, which are at least necessary for describing the third-order nonlinear optical processes. The transition dipole matrix element ($\mu^{\mathrm{agg}}_{ll'}$) in the direction of the applied field for this new state model are also calculated. It is noted that only the transition moments between the ground (1) and the one-exciton states l ($l = 2,\ldots,N+1$) and those between the two-exciton states l' ($l' = N+2,\ldots,M$) and the one-exciton states exist in the two-exciton model.

TIME EVOLUTION OF AN M-STATE AGGREGATE MODEL INTERACTING WITH A SINGLE-MODE QUANTIZED FIELD

We consider a general M-state molecule model ($M \geq 2$, integer) in a single-mode photon field. The total Hamiltonian H is represented by [24]

$$H = H_{\mathrm{agg}} + H_{\mathrm{field}} + H_{\mathrm{int}} = \sum_{l=1}^{M} E^{\mathrm{agg}}_l b^+_l b_l + \left(c^+c + \frac{1}{2}\right)\hbar\omega + \left(\frac{\hbar\omega}{2\varepsilon_0 V}\right)^{1/2}\sum_{l,l'=1}^{M}\mu^{\mathrm{agg}}_{ll'}b^+_l b_{l'}(c+c^+), \quad (2)$$

where the first (H_{agg}), second (H_{field}), and third (H_{int}) terms on the right side represent the unperturbed molecular aggregate system, the single-mode photon field, and their interaction, respectively. In the second term, ω the frequency of the single-mode photon field, and c^+ and c are the creation and annihilation operators for the single-mode photon field. In the third term, V is the volume of the cavity containing the single-mode photon field and it is fixed to 10^7 Å^3 in this study. The matrix elements of the above Hamiltonian are obtained by using a double Hilbert space spanned by the molecular states $\{|\Psi^{\mathrm{agg}}_l\rangle\}$ ($l = 1,2,\ldots,M$) and the photon number states $\{|m\rangle\}$ ($m = 0,1,2,\ldots,\infty$) [24]. Using the eigenvalues $\{W(m)\}$ and eigenvectors $\{\chi(m)\}$ ($m = 0,1,2,\ldots$) of the Hamiltonian [Eq. (2)], the matrix element of the time-evolution operator, $U(t,t_0)$, is represented by

$$\langle j;n|U(t,t_0)|j';n'\rangle \equiv U_{j,n;j',n'} = \sum_m \langle j;n|\chi(m)\rangle\langle\chi(m)|j';n'\rangle \times e^{-iW(m)(t-t_0)/\hbar}, \quad (3)$$

where j and n specify the molecular aggregate state and the photon number state, respectively. The observable properties of photons and molecules are described by using the density matrix:

$$\langle j;n|\rho(t)|j';n'\rangle \equiv \rho_{j,n;j',n'}(t)\sum_{f,g}^{M}\sum_{m,m'} U_{j,n;f,m}(t,t_0) \times \rho_{f,m;g,m'}(t_0)U^+_{g,m';j',n'}(t,t_0). \quad (4)$$

In our procedure, we first construct an initial density matrix ($\rho_{f,n;g,n'}(t_0) = \rho^{\mathrm{agg}}_{f,g}(t_0)\rho^{\mathrm{phot}}_{n,n'}(t_0)$). The initial aggregate state is assumed to be the ground state and the initial photon field is assumed to be in a single-mode coherent state. The probability distribution of finding n photons in this state is a Poisson distribution. The elements of the initial photon field density matrix are represented by

$$\rho^{\mathrm{phot}}_{n,n'}(t_0) = \frac{\langle\hat{n}\rangle^{(n+n')/2}e^{-\langle\hat{n}\rangle}}{\sqrt{n!n'!}}, \quad (5)$$

where $\langle\hat{n}\rangle$ is the mean number of photons in the coherent state. Second, the density matrix elements ($\rho_{\gamma,n;\gamma',n'}(t)$) at time t are calculated by using Eqs. (3) and (4). Third, the molecular and photon reduced density matrix elements are obtained by $\rho^{\mathrm{agg}}_{\gamma,\gamma'}(t) = \sum_n \rho_{\gamma,n;\gamma',n}(t)$ and $\rho^{\mathrm{phot}}_{n,n'}(t) = \sum_\gamma \rho_{\gamma,n;\gamma,n'}(t)$, respectively. Finally, various properties concerning the photons and the molecule are calculated by using these density matrices.

PHOTON-PHASE PROPERTIES BY USING THE PEGG–BARNETT (PB) OPERATOR AND AGGREGATE ENTROPY

The phase properties of a single-mode photon field have been investigated by the Pegg–Barnett (PB) operator. In this approach, all calculations concerning the phase properties are performed in an $(s+1)$-dimensional space spanned by $s+1$ orthonormal phase states, and the s value will be taken to be infinity after all the expectation values have been calculated. The $s+1$ orthonormal phase states are defined by

$$|\phi_m\rangle = \frac{1}{\sqrt{s+1}} \sum_{n=0}^{s} \exp(in\phi_m)|n\rangle, \qquad (6)$$

where

$$\phi_m = \phi_0 + \frac{2\pi m}{s+1} \qquad (m = 0, 1, 2, \ldots, s). \qquad (7)$$

Here, $|n\rangle$ is the photon number state, and ϕ_0 is an arbitrary real number. In this article, we adopt $\phi_0 = -s\pi/(s+1)$ to locate the initial phase of a single-mode coherent photon field on the origin ($\phi = 0$) of the phase axis defined in the region: $-\pi \le \phi_m \le \pi$. Pegg and Barnett defined the following Hermitian phase operator $\hat{\phi}$ [13–15] to provide an eigenvalue ϕ_m and an eigenstate $|\phi_m\rangle$. The expectation values of arbitrary functions of phase operator $f(\hat{\phi})$ for arbitrary physical states $|\psi\rangle$ can be calculated by

$$\langle f(\hat{\phi})\rangle = \lim_{s\to\infty} \langle\psi|f(\hat{\phi})|\psi\rangle = \lim_{s\to\infty} \sum_{m=0}^{s} f(\phi_m)P(\phi_m) \quad (8)$$

where $P(\phi_m)$ is a phase distribution function, which represents the probability that the phase of a physical state $|\psi\rangle$ is ϕ_m. Using Eqs. (6) and (7), the phase distribution function can be expressed by

$$P(\phi_m, t) = \frac{1}{s+1} \sum_{n,n'=0}^{s} \exp\left[i(n-n')\phi_m\right]\rho_{n',n}^{\mathrm{phot}}(t). \quad (9)$$

By using Eqs. (8) and (9), we calculate $P(\phi_m)$, $\langle\cos^2\hat{\phi}\rangle$ and $\Delta\cos^2\phi$ for some molecule–photon field coupled systems at time t. In the present numerical calculations, s is taken to be 400. It is noted that the time t is taken as $2\pi m/\omega$ ($m = 0, 1, 2, \ldots$) to remove the phase (ωt) of the free field.

The information entropy of a molecular aggregate (aggregate entropy) is defined by

$$S^{\mathrm{agg}} = -\mathrm{Tr}\left(\rho^{\mathrm{agg}} \ln \rho^{\mathrm{agg}}\right) = -\sum_{i=1}^{M} \rho_{ii}^{\mathrm{agg}'} \ln\left(\rho_{ii}^{\mathrm{agg}'}\right), \qquad (10)$$

where $\rho_{ii}^{\mathrm{agg}'}$ is the diagonalized aggregate reduced density matrix. For a pure state, $S^{\mathrm{agg}} = 0$, while, for a mixed state, $S^{\mathrm{agg}} > 0$. Namely, the time evolution of the aggregate entropy reflects the time evolution of the degree of entanglement between the molecular aggregate and the field. The larger the entropy, the greater the entanglement.

Results and Discussion

ONE- AND TWO-EXCITON DIMER STATE MODELS WITH DIFFERENT INTERMOLECULAR DISTANCES

Figures 2(O-a)–(O-d) and 2(T-a)–(T-d), respectively, show one- and two-exciton dimer state models with different intermolecular distances (R): (a) $R = \infty$ a.u. (noninteracting case), (b) $R = 12$ a.u., (c) $R = 10$ a.u., and (d) $R = 8$ a.u. As is well known, the intermolecular interaction in H-aggregate-type dimer significantly increases the first excitation energy (E_{21}^{agg}) when the intermolecular distance becomes small. This is due to a strong interaction between the one-exciton states $|12\rangle$ and $|21\rangle$, which construct the first excited state $|\Psi_2^{\mathrm{agg}}\rangle$. On the other hand, the second excitation energy (E_{31}^{agg}) does not exhibit a remarkable change since the interaction between the two-exciton state $|22\rangle$ and the nonexciton state $|11\rangle$ is weak due to the large energy separation between them. Therefore, the $|\Psi_1^{\mathrm{agg}}\rangle$ and $|\Psi_3^{\mathrm{agg}}\rangle$ of the two-exciton model are well approximated to be $|11\rangle$ and $|22\rangle$, respectively. In the case of applying the resonant field with respect to the excited state of monomer, we observe a large deviation of the first excitation energy (E_{21}^{agg}) of dimer from the monomer excitation energy ($E_{21} = 37800\ \mathrm{cm}^{-1}$) in contrast to the case of the second excitation energy (E_{31}^{agg}). This feature is expected to enhance the contribution of the two-photon process between the ground and the second excited states of dimer [26].

TIME EVOLUTION OF DIMER DENSITY MATRICES, PHOTON-PHASE PROPERTIES, AND DIMER ENTROPY FOR ONE- AND TWO-EXCITON MODELS

Below, we elucidate the differences in the features of quantum dynamics of exciton population between the one- and two-exciton models from the viewpoint of the photon-phase and molecular-entropy dynamics.

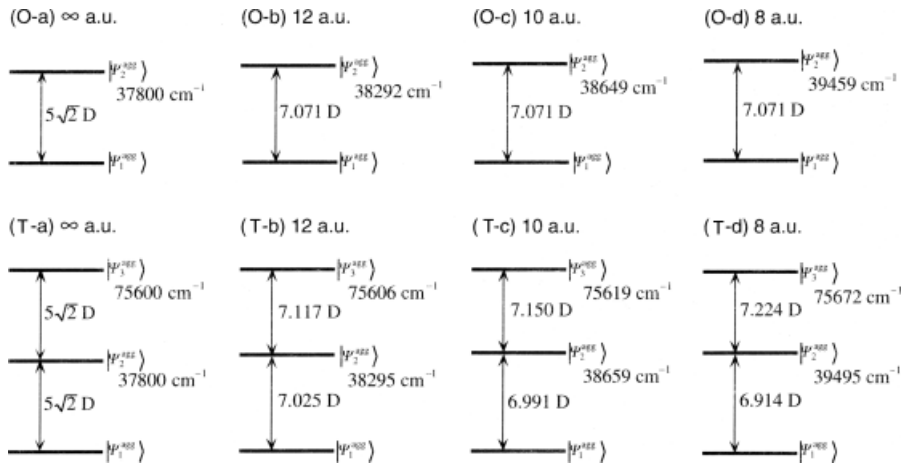

FIGURE 2. State models of *H*-aggregate-type molecular dimers shown in Figure 1 with several intermolecular distances (R): (O-a) $R = \infty$ a.u., (O-b) $R = 12$ a.u., (O-c) $R = 10$ a.u., and (O-d) $R = 8$ a.u. for the one-exciton model: (T-a) $R = \infty$ a.u., (T-b) $R = 12$ a.u., (T-c) $R = 10$ a.u., and (T-d) $R = 8$ a.u. for the two-exciton model.

Collapse-Revival Behavior of Diagonal Dimer Density Matrices

The resonant frequency of a single-mode coherent photon field (average photon number $\langle \hat{n} \rangle = 8$) is 37800 cm^{-1}. Figures 3(d-O-a)–(d-O-d) and 4(d-T-a)–(d-T-d) show the time evolution of diagonal density matrices of dimers, $\rho_{1,1;1,1}(t)$, $\rho_{1,2;1,2}(t)+\rho_{2,1;2,1}(t)$ (one-exciton population) and $\rho_{2,2;2,2}(t)$ (two-exciton population which only exists for two-exciton model), with several intermolecular distances. The mechanism and the features of a peculiar behavior, i.e., the damped oscillations (collapses) and the amplified oscillations (revivals) in dimer density matrices, have been well analyzed [1–10], and then the collapse is found to originate in the dephasing among Rabi oscillations with slightly different frequencies, while the revival is found to originate in the rephasing observed in quantum systems with a small number of degrees of freedom. Although similar time-evolution behavior, i.e., collapse-revival behavior, of the ground dimer density matrices, $\rho_{1,1;1,1}(t)$, is observed for these dimer models, some differences in the collapse-revival behavior are detected between the one- and two-exciton models and are also observed among the models with different intermolecular distances. It is found that the first revival-collapse behavior in the one-exciton model begins later than that in the two-exciton model at each intermolecular distance, and that the amplitude of the first revival-collapse behavior is shown to be much smaller than that of the second one in the two-exciton model [see, for example, Fig. 4(d-T-a)], while the amplitudes of the first revival-collapse are slightly larger than the second one in the one-exciton model [see, for example, Fig. 3(d-O-a)]. It is found for the one-exciton models that as the intermolecular distance becomes small, the revival times (at which the amplitude of revival oscillation takes a local maximum value) become large, and the first and the second revival-collapse amplitudes become small. By contrast, it is found for the two-exciton models that as the intermolecular distance reduces, the revival times become large and the first revival-collapse amplitude becomes small, while the second revival-collapse amplitude becomes large. The decrease in the magnitude of $\rho_{1,1;1,1}(t)$ with the decrease in the intermolecular distance indicates the enhancement of the deviation of the first excitation energy E_{21}^{agg} from the monomer excitation energy E_{21}^{k} due to the increase in the intermolecular interaction. It is found that the first revival-collapse oscillation of $\rho_{1,1;1,1}(t)$ is mainly contributed by the one-exciton population $\rho_{1,2;1,2}(t) + \rho_{2,1;2,1}(t)$ both in the one- and two-exciton models, while the second revival-collapse oscillation of $\rho_{1,1;1,1}(t)$ in the two-exciton model is mainly contributed by the two-exciton population $\rho_{2,2;2,2}(t)$, which is generated by the two-photon process in the three-state model shown in Figure 2(T-a)–(T-d), although the second revival-collapse oscillation of $\rho_{1,1;1,1}(t)$ in the one-exciton model is contributed by one-exciton population, $\rho_{1,2;1,2}(t)+\rho_{2,1;2,1}(t)$. Namely, the variation in the first and the second revival-collapse amplitudes of $\rho_{1,1;1,1}(t)$ in the two-exciton models with small intermolecular distances is ex-

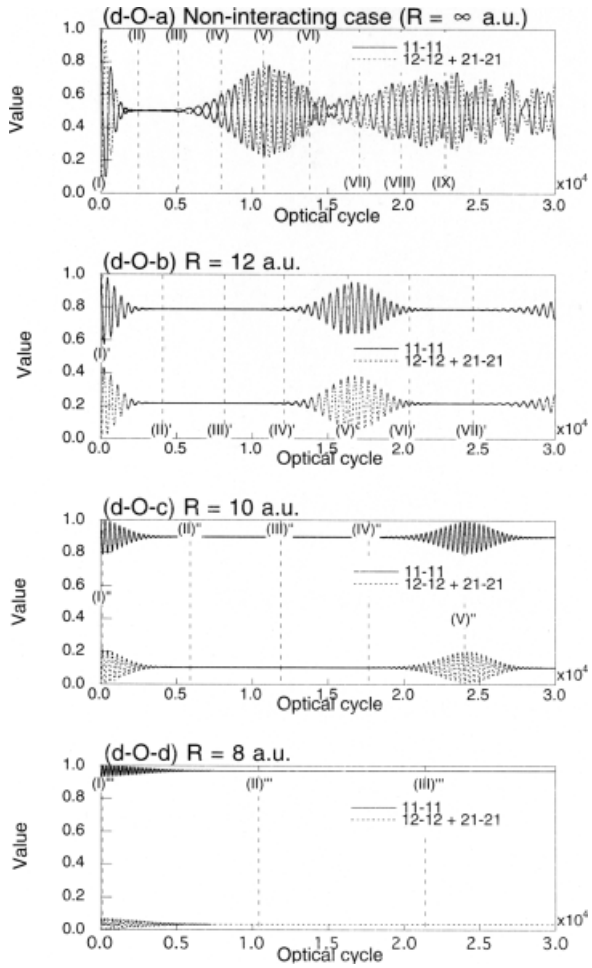

FIGURE 3. Time evolution of the ground ($\rho^{agg}_{1,1;1,1}(t)$) and the one-exciton ($\rho^{agg}_{1,2;1,2}(t) + \rho^{agg}_{2,1;2,1}(t)$) populations for the one-exciton models (Fig. 2) with several intermolecular distances (R): (d-O-a) $R = \infty$ a.u., (d-O-b) $R = 12$ a.u., (d-O-c) $R = 10$ a.u., and (d-O-d) $R = 8$ a.u. 11-11 and 12-12 + 21-21 represent $\rho^{agg}_{1,1;1,1}(t)$ and $\rho^{agg}_{1,2;1,2}(t) + \rho^{agg}_{2,1;2,1}(t)$, respectively. The unit of optical cycle is $2\pi/m\omega$ [a.u.] (m: division number = 8).

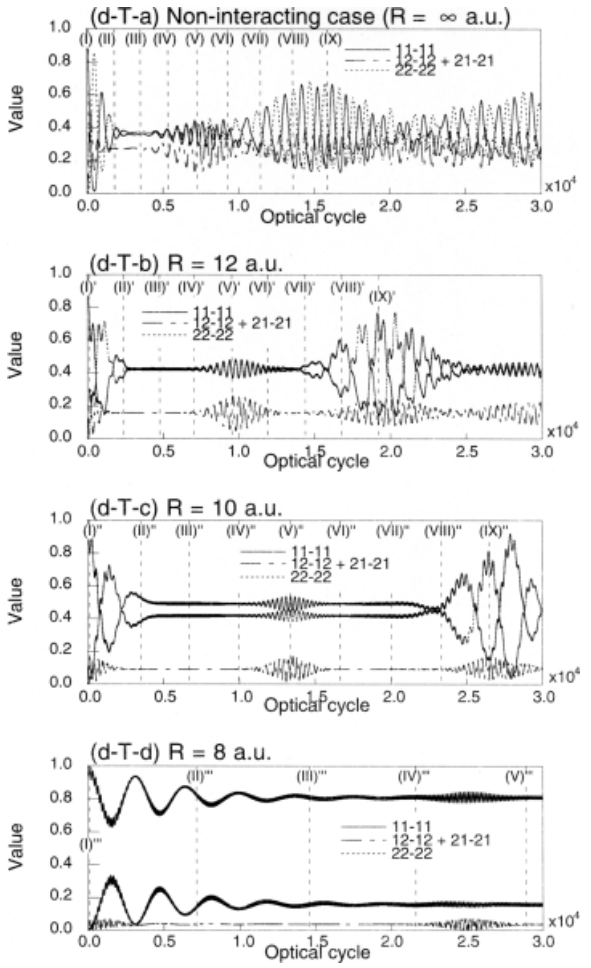

FIGURE 4. Time evolution of the ground ($\rho^{agg}_{1,1;1,1}(t)$), the one-exciton ($\rho^{agg}_{1,2;1,2}(t) + \rho^{agg}_{2,1;2,1}(t)$) and the two-exciton ($\rho^{agg}_{2,2;2,2}(t)$) populations for the two-exciton models (Fig. 2) with several intermolecular distances (R): (d-T-a) $R = \infty$ a.u., (d-T-b) $R = 12$ a.u., (d-T-c) $R = 10$ a.u., and (d-T-d) $R = 8$ a.u. 11-11, 12-12 + 21-21, and 22-22 represent $\rho^{agg}_{1,1;1,1}(t)$, $\rho^{agg}_{1,2;1,2}(t) + \rho^{agg}_{2,1;2,1}(t)$, and $\rho^{agg}_{2,2;2,2}(t)$, respectively. The unit of optical cycle is $2\pi/m\omega$ [a.u.] (m: division number = 8).

plained by the increase in the contribution of two-photon process due to the significant changes in the first excited-state energy with increasing intermolecular interaction in contrast to the second excited state energy [see Fig. 2(T-a)–(T-d)].

Dimer Entropy and Photon-Phase Properties

Dimer entropy S^{agg} for (O-a)–(O-d) and (T-a)–(T-d) are shown in Figures 5 and 6, respectively. The photon-phase properties ($\langle \cos^2 \hat{\phi} \rangle$ and $\Delta \cos^2 \phi$) for these systems are shown in Figures 7 and 8. The dotted lines (I)–(IX), etc., shown in Figures 3–10 indicate the time at which the $\langle \cos^2 \hat{\phi} \rangle$ takes local minimum, local maximum, and their intermediate values.

The magnitude of S^{agg}, which represents the degree of the correlation (entanglement) between dimer and photon, is shown to become small as the intermolecular distance is small since the degree of off-resonance with respect to the first excited state $|\Psi^{agg}_2\rangle$ increases. It is well known in a molecule-coherent field coupled system that the molecular entropy increases first and then decreases to the local

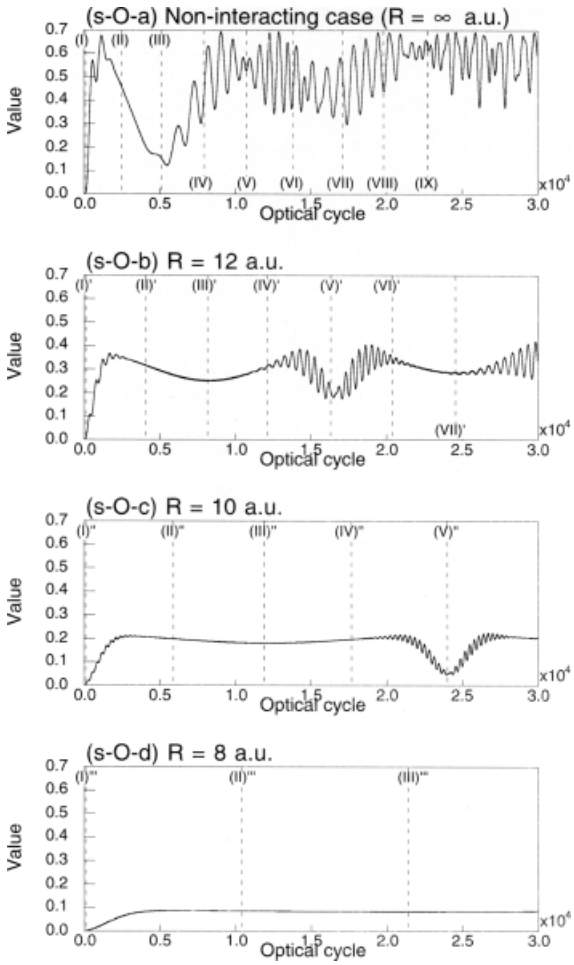

FIGURE 5. Time evolution of the information entropy of dimers ($S^{agg}(t)$) for the one-exciton models (Fig. 2) with several intermolecular distances (R): (s-O-a)–(s-O-d). At the initial time, the dimer is assumed to be in the ground state, and the photon field is in a single-mode coherent state ($\langle\hat{n}\rangle = 8$, $\omega = 37{,}800\ \mathrm{cm}^{-1}$). The unit of optical cycle is $2\pi/m\omega$ [a.u.] (m: division number $= 8$).

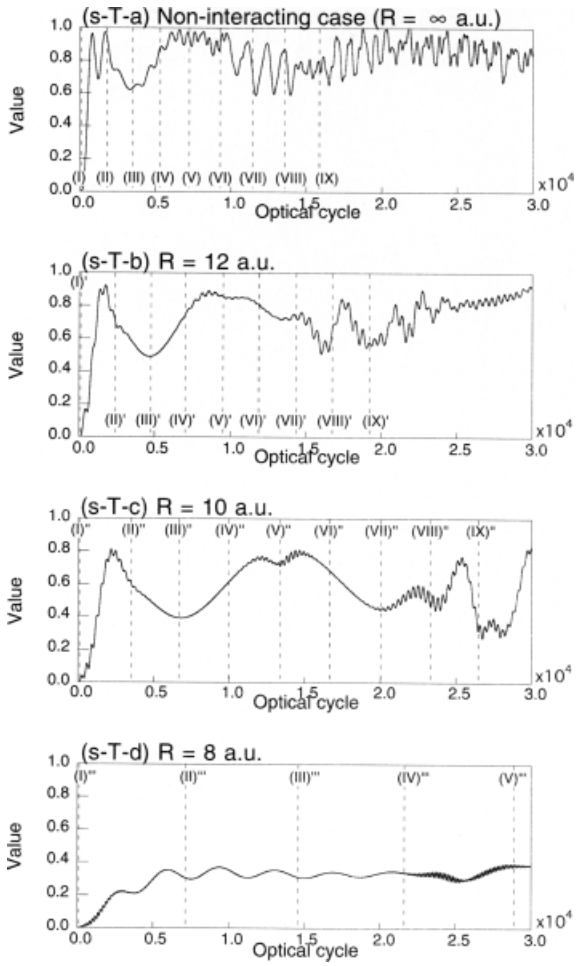

FIGURE 6. Time evolution of the information entropy of dimers ($S^{agg}(t)$) for the two-exciton models with several intermolecular distances: (s-T-a)–(s-T-d). See Figure 5 for further legends.

minimum value in the first collapse and subsequent quiescent regions [5]. The minimum S^{agg} at the half-revival time implies that nearly pure molecular state (which is a coherent superposition of the two energy state of the molecule) is created momentarily, while the photon field generates a Schrödinger-cat state, macroscopic superposition state, of two coherent field states with mutually opposite phases ($\pi/2$ and $-\pi/2$). Although both exciton models exhibit similar significant decreases in S^{agg} in the quiescent regions for noninteracting cases, the decrease in S^{agg} in the one-exciton model is more remarkable than that in the two-exciton model. It is further found that as the intermolecular distance becomes small, the decrease in S^{agg} in the one-exciton models rapidly disappear, while that in the two-exciton model exhibits only a slight change for relatively small intermolecular distances [see Fig. 6(s-T-b) and (s-T-c)].

In general, the collapses and revivals behavior of molecular population closely relates to the time-evolution behavior of photon-phase properties [16–24]. All the $\langle\cos^2\hat{\phi}\rangle$ exhibit damped oscillations (see Figs. 8 and 9). The amplitude of the damped oscillation of $\langle\cos^2\hat{\phi}\rangle$ is shown to become large as the intermolecular distance becomes small. The $\Delta\cos^2\phi$ are found to oscillately increase in the one-exciton models, while in the two-exciton model the $\Delta\cos^2\phi$ are found to behave damped oscillately with the largest values at time (V) [(V)′, (V)″, and

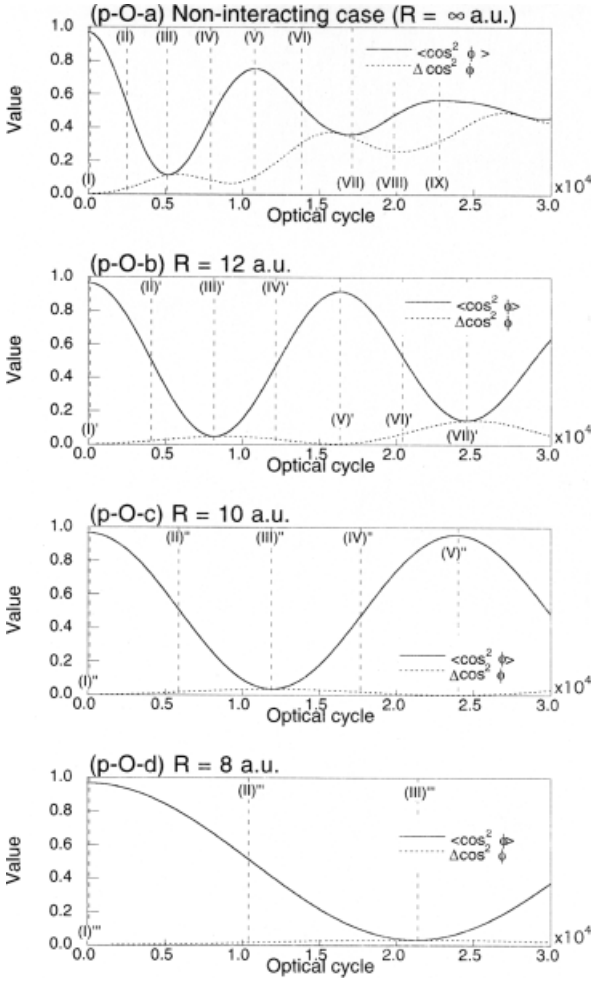

FIGURE 7. Time evolution of the photon-phase properties ($\langle \cos^2 \hat{\phi} \rangle$ and $\Delta \cos^2 \phi$) for the one-exciton models (Fig. 2) with several intermolecular distances (R): (p-O-a)–(p-O-d). It is noted that (I) [(I)′, (I)″, and (I)‴], (III) [(III)′, (III)″, and (III)‴], etc., represent the times at which $\langle \cos^2 \hat{\phi} \rangle$ takes local maximum and local minimum values, respectively, for each dimer model. The intermediate times are represented by (II) [(II)′, (II)″, and (II)‴], (IV) [(IV)′, (IV)″, and (IV)‴], etc. The unit of optical cycle is $2\pi/m\omega$ [a.u.] (m: division number = 8).

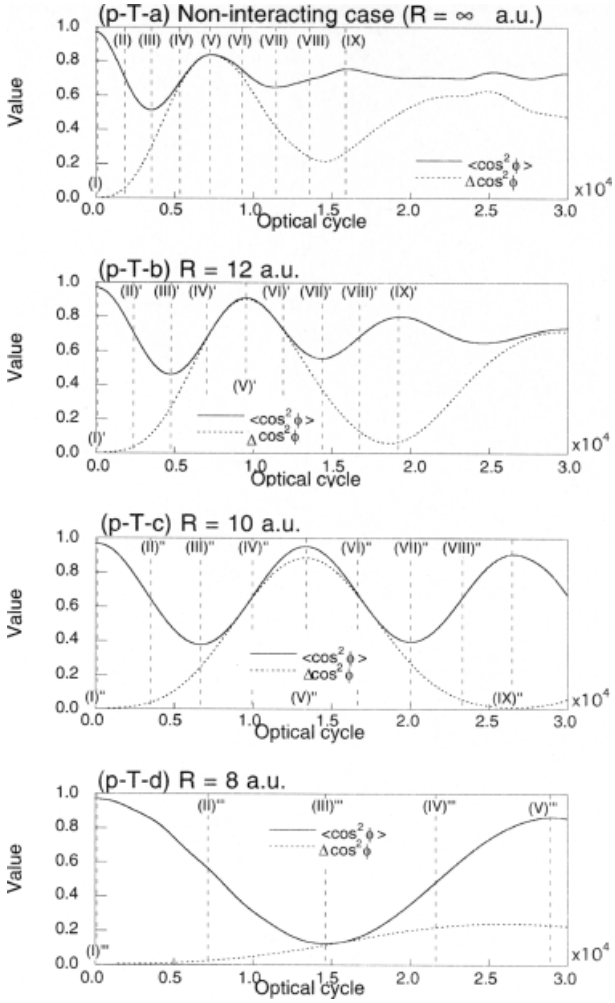

FIGURE 8. Time evolution of the photon-phase properties ($\langle \cos^2 \hat{\phi} \rangle$ and $\Delta \cos^2 \phi$) for the two-exciton models (Fig. 2) with several intermolecular distances (R): (p-T-a)–(p-T-d). See Figure 7 for further legends.

(V)‴]. These differences are found to originate in the differences in the dynamics of photon-phase distribution between two- and three-state systems. Details of the relation among the state-model systems and the behavior of $\langle \cos^2 \hat{\phi} \rangle$ and $\Delta \cos^2 \phi$ are discussed in our previous papers [18–24].

Pegg-Barnett Photon-Phase Distribution

In order to more elucidate the photon-phase dynamics, we investigate PB photon-phase distributions at each time for noninteracting and interacting cases: (O-a), (O-b), and (O-d) for the one-exciton models, and (T-a), (T-b), and (T-d) for the two-exciton models. These results are shown in Figures 9 and 10. Both photon-phase distribution dynamics for the one- and two-exciton models show the splitting of the initial single peak and subsequent moving in the mutually opposite direction. Such photon-phase splitting is known to be caused by the interaction between the molecule and a relatively small number of photons [16–24]. It was found that the early separation of photon-phase distribution with $|\phi| \leq \pi/2$ causes the increase in the ability of destructing the coherency (the definite relative phase relation) between the ground and the

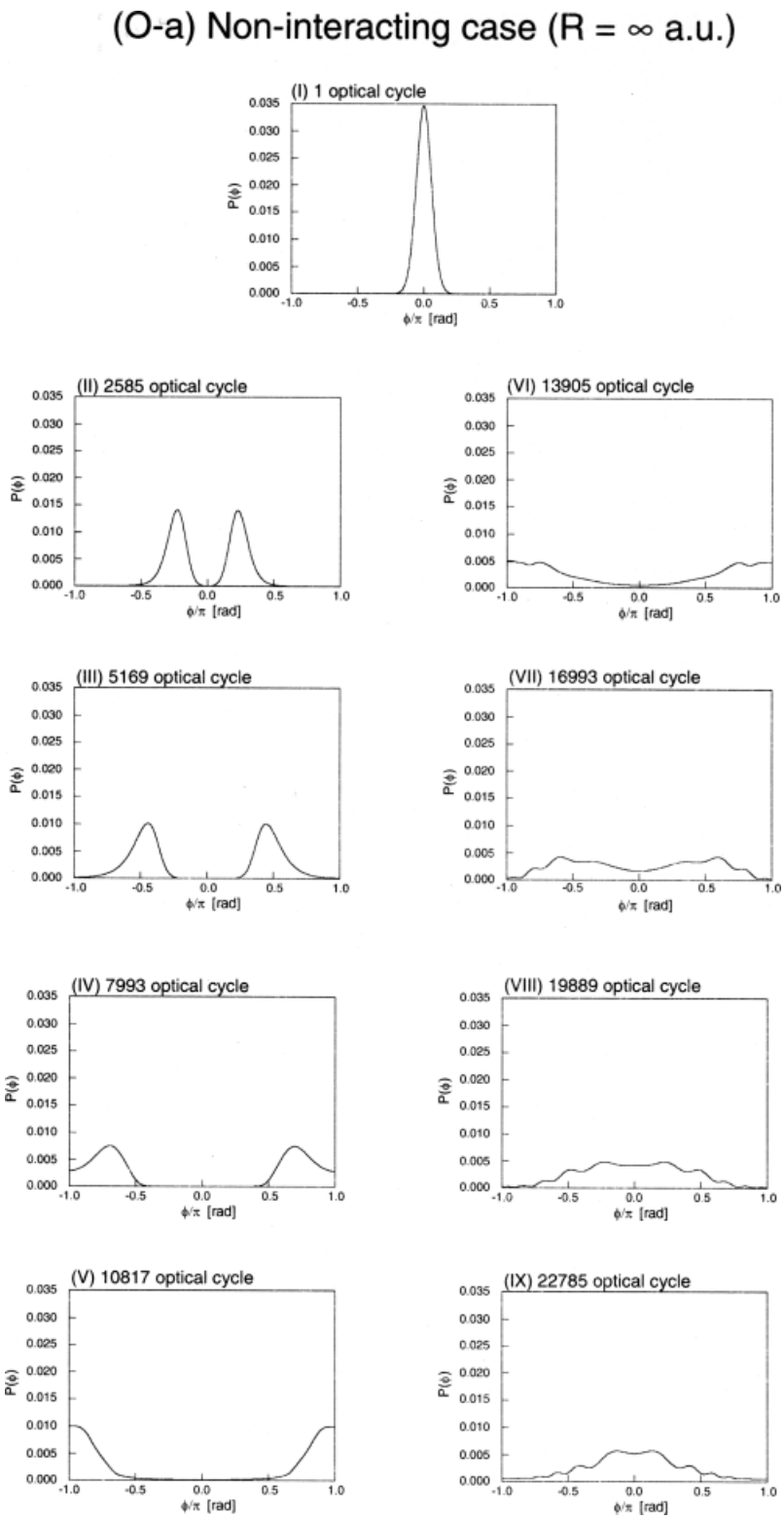

FIGURE 9. Pegg–Barnett (PB) photon-phase distributions at times (I), (II), etc. (shown in Fig. 7) for the one-exciton models (Fig. 2) with several intermolecular distances (R): (O-a), (O-b), and (O-d). In the present numerical calculations, s in Eq. (6) is taken to be 400. The unit of optical cycle is $2\pi/m\omega$ [a.u.] (m: division number = 8).

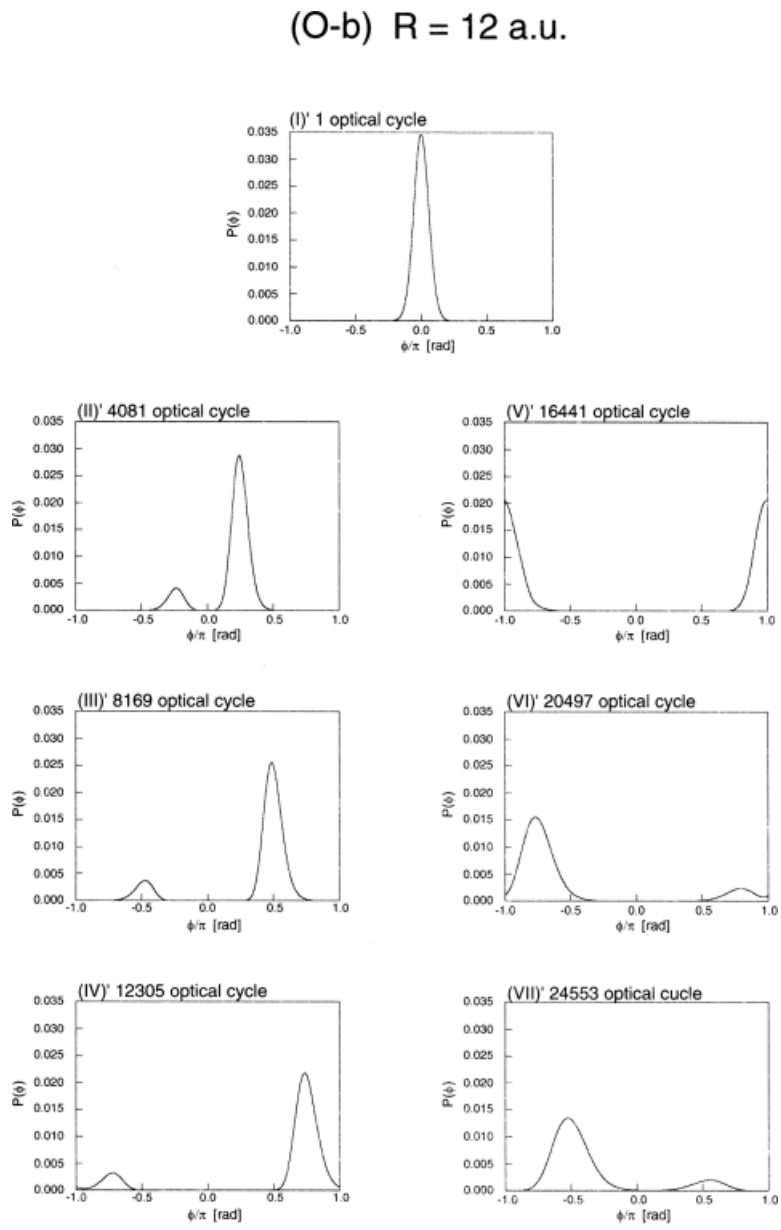

FIGURE 9. (Continued)

excited states of molecule and the further separation (split peaks approach $\pm\pi/2$, respectively) decreases such ability, so that the degree of entanglement between molecule and photon first increases and then decreases in the first collapse region [5]. This variation in the degree of entanglement corresponds to the magnitude of variation in S^{agg}. A significant difference in the photon-phase distribution dynamics between the one- and two-exciton models is the number of split peaks. The one-exciton model exhibits the splitting to two peaks, while the two-exciton model does to the three peaks involving a standing central peak. This feature is found to be related to the number of molecular states considered [18]. In general, odd- and even-numbered state models are predicted to provide odd- and even-numbered split peaks [18]. Another interesting point is the effects of intermolecular distance on the relative intensity of the split peaks and their dynamics. As shown in Figure 2, the noninteracting

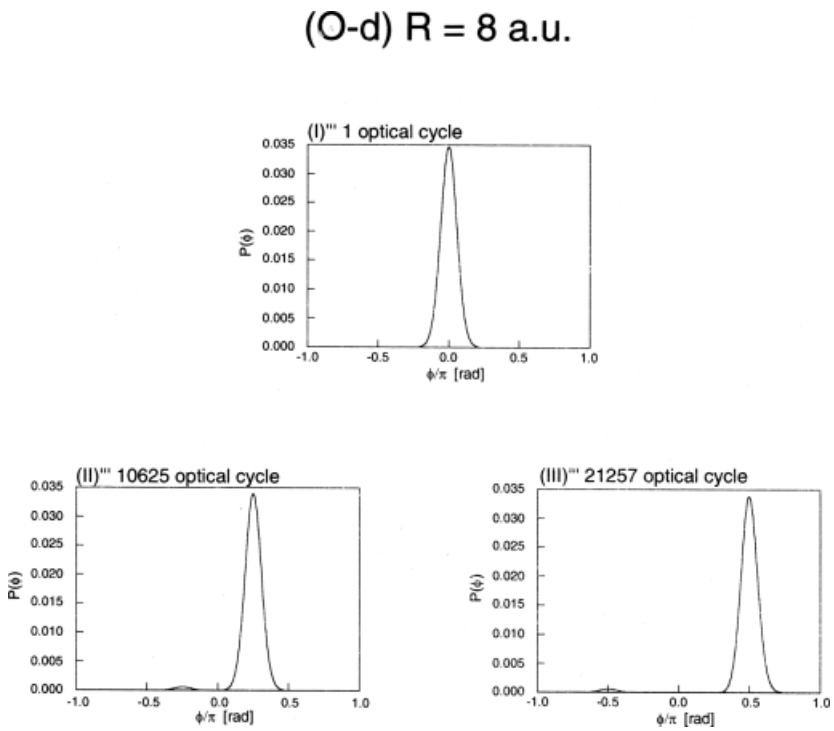

FIGURE 9. (Continued)

cases [(O-a) and (T-a)] correspond to the resonant case, while the intensity of intermolecular interaction increases the degree of the off-resonance with respect to the applied field ($\omega = 38000$ cm^{-1}). For the noninteracting one-exciton model case (O-a), the two split peaks are found to be identical, while for the slightly off-resonant case (O-b), the peak intensity in the positive phase region is larger than that in the negative phase region. Further off-resonance is shown to almost extinguish the split peak in the negative phase region and to cause a moving of a single split peak [see Fig. 9(O-d)]. Such difference in the intensities of the split distribution peaks with respect to the degree of resonance originates in the difference in the absorption of photons [18]. It is found from these phase-distribution dynamics in the one-exciton model that the degree of the photon-phase separation becomes smaller as the intermolecular interaction increases. Namely, the ability of the destroying the relative phase between aggregate ground and excited states reduces as the intermolecular interaction increases. This corresponds to the disappearance of the distinct decrease in S^{agg} about at $\phi = \pm\pi/2$. In contrast, for three split peaks in noninteracting two-exciton model (T-a), the both-side peak intensities are found to be identical and are smaller than that of the central peak [18, 20, 24]. In the slightly off-resonant case (T-b), the peak intensity in the positive phase region is larger than that in the negative phase region. This feature leads to a larger separation of phase distribution in the slightly off-resonant cases, e.g., (T-b) and (T-c), compared to the resonant case (T-a). In the further off-resonant case (T-d), split peaks hardly appear since the degree of splitting relates to the intensity of the coupling between aggregate and photon. These differences in splitting behavior correspond to the significant differences in S^{agg} in the first quiescent region between (T-b) and (T-d) [see Fig. 6(s-T-b) and (s-T-d)]. The disappearance of the phase split for (T-d) corresponds to the slight change in S^{agg} for (T-d). It is noted for the one- and two-exciton models that the enhancement of revival time (Figs. 3 and 4), slow variation in phase properties (Figs. 7 and 8), and slow splitting of phase peak (Figs. 9 and 10) in the small intermolecular distance (larger intermolecular interaction) case reflect the decrease in the aggregate-photon correlation.

Off-Diagonal Dimer Density Matrices in the Two-Exciton Model

It is found from the dynamics of photon-phase and diagonal aggregate density matrices that the

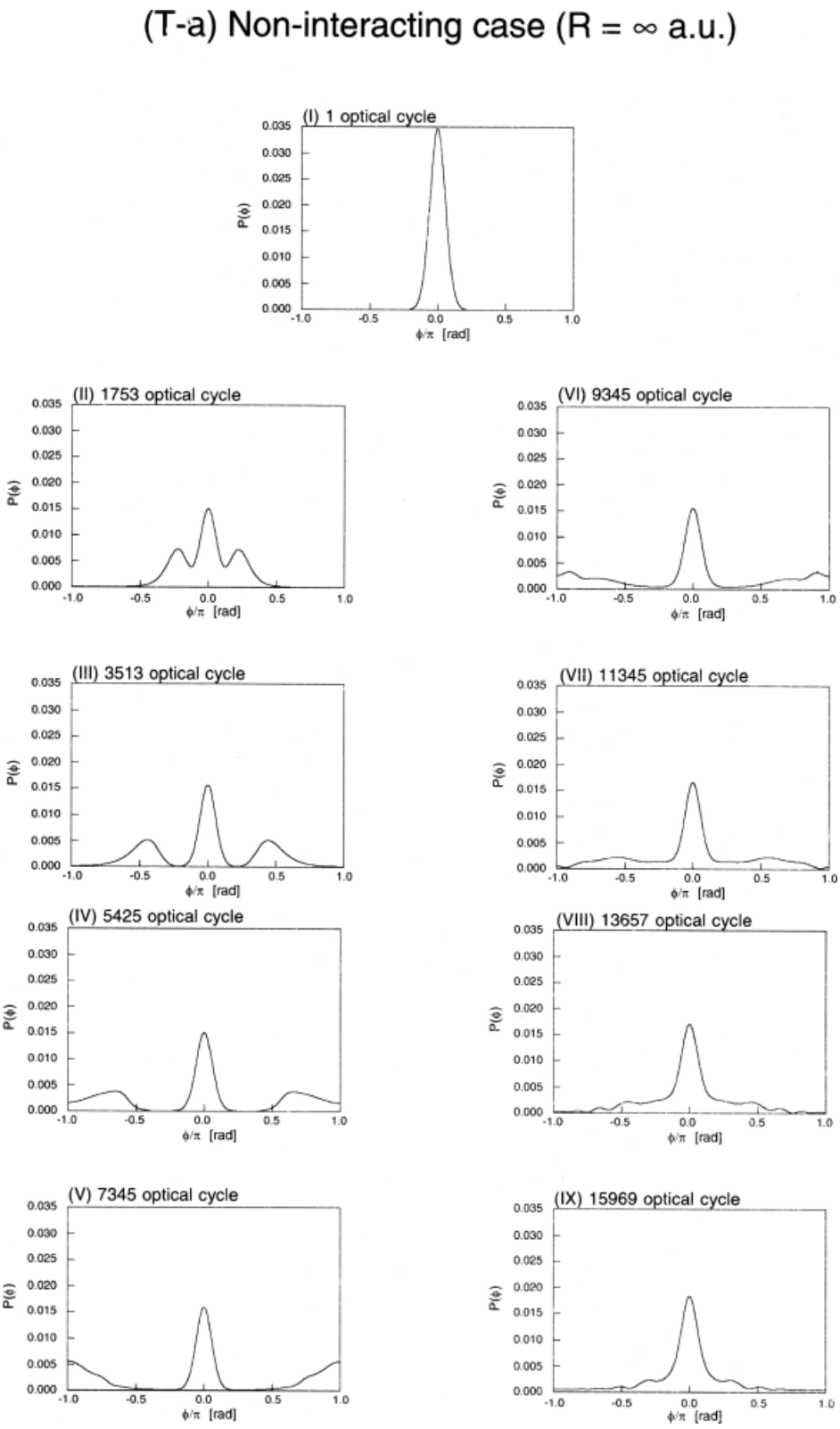

FIGURE 10. Pegg–Barnett (PB) photon-phase distributions at times (I), (II), etc. (shown in Fig. 8) for the two-exciton models (Fig. 2) with several intermolecular distances (*R*): (T-a), (T-b), and (T-d). See Figure 9 for further legends.

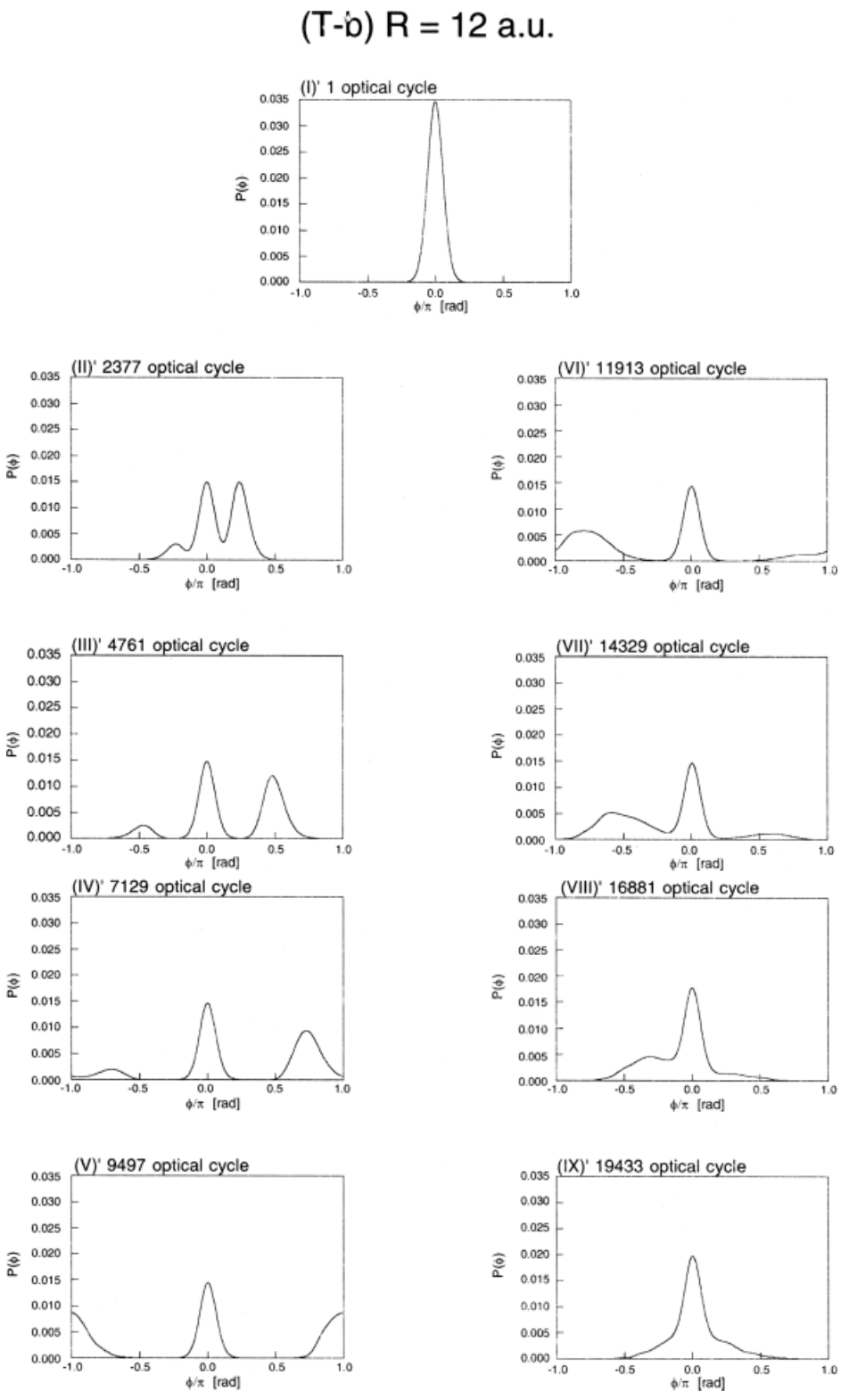

FIGURE 10. (Continued)

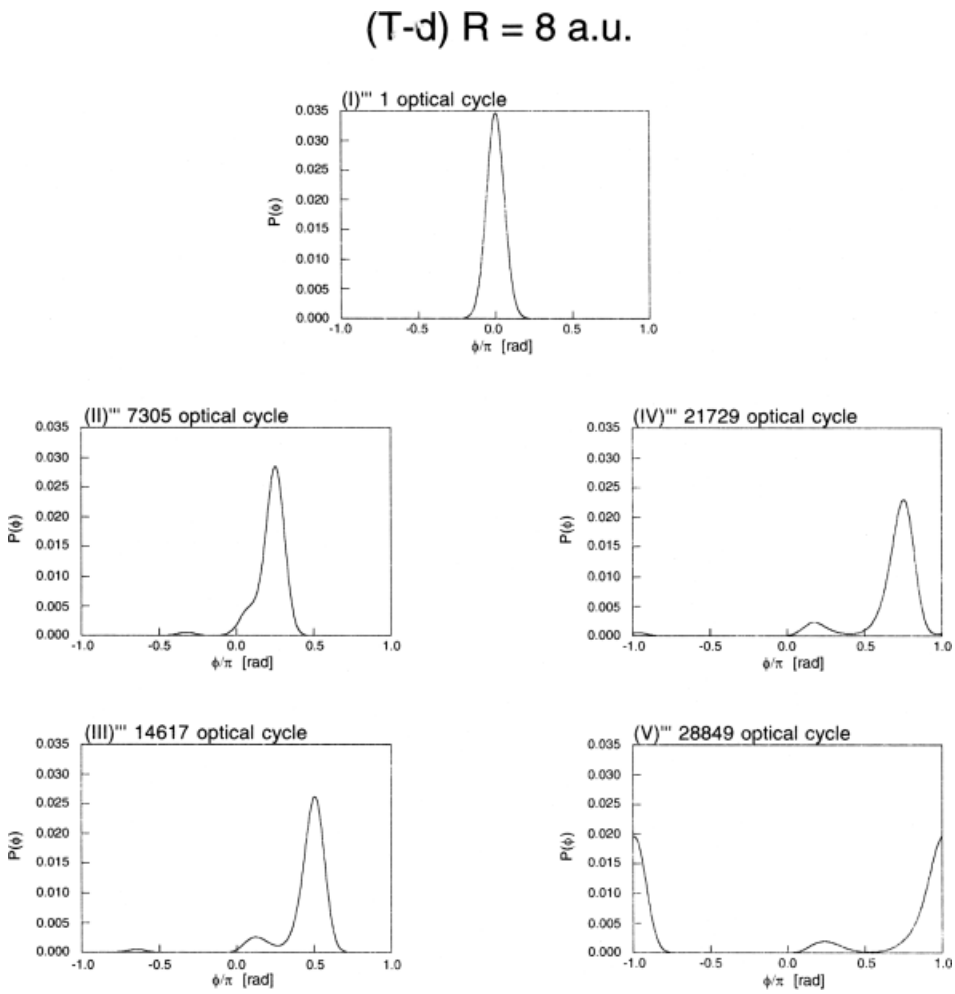

FIGURE 10. (Continued)

differences in dynamics between the one- and two-exciton models originate in the existence of a two-photon process between the ground and the second excited states in the two-exciton model. Namely, in the case of the applied field which is resonant or near-resonant with the first excited state, the inclusion of two-exciton states is found to be essential for describing the qualitative features of the dynamics of dimer models composed of two-state monomers. In this section, we investigate the dynamics of off-diagonal matrix elements among aggregate states in the two-exciton model to elucidate the variation in the relative phase (coherence) between the states with respect to the variation in the photon-phase dynamics.

Figure 11 shows the time evolution of the magnitude of off-diagonal density matrix elements, $\rho_{1,1;1,2}(t)+\rho_{1,1;2,1}(t)$, $\rho_{1,2;2,2}(t)+\rho_{2,1;2,2}(t)$, and $\rho_{1,1;2,2}(t)$, for the two-exciton model. As expected from the variation in S^{agg} (Fig. 6), the magnitude of $\rho_{1,1;2,2}(t)$ enhances in the first and the second quiescent regions, e.g., (II)″–(IV)′ and (VI)′–(VIII)′ for (T-b) (see also Fig. 2), respectively. This indicates that the phase relation between $|\Psi_3^{\mathrm{agg}}\rangle$ and $|\Psi_1^{\mathrm{agg}}\rangle$ becomes more definite in the quiescent regions due to the increase in the degree of disentanglement between photon and aggregate. It is noted that such anomalous behavior, i.e., changes in off-diagonal density matrices without changes in diagonal density matrices, cannot be achieved by classical laser field and is useful for controlling only the quantum phase properties [23]. By comparison between the phases in the first and the second revival-collapse oscillations of off-diagonal density matrices, the first quiescent and revival-collapse regions are found to be constructed from two simultaneous one-photon processes: $|\Psi_3^{\mathrm{agg}}\rangle - |\Psi_2^{\mathrm{agg}}\rangle - |\Psi_3^{\mathrm{agg}}\rangle$ and $|\Psi_1^{\mathrm{agg}}\rangle - |\Psi_2^{\mathrm{agg}}\rangle - |\Psi_1^{\mathrm{agg}}\rangle$; while

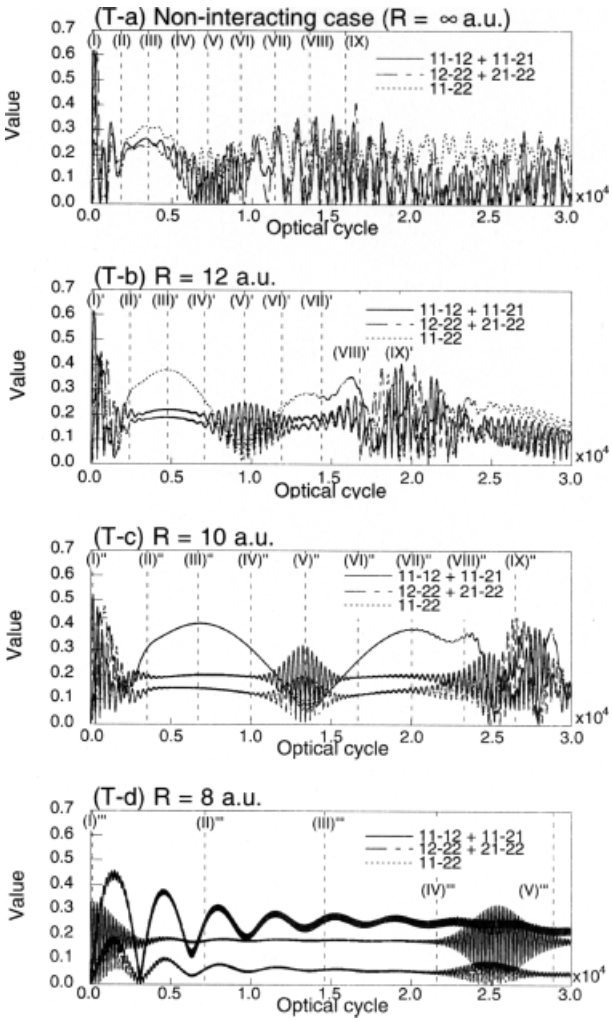

FIGURE 11. Time evolution of the magnitude of off-diagonal aggregate density matrices: $\rho^{agg}_{1,1;1,2}(t) + \rho^{agg}_{1,1;2,1}(t)$, $\rho^{agg}_{1,1;2,2}(t)$, $\rho^{agg}_{1,2;2,2}(t) + \rho^{agg}_{2,1;2,2}(t)$, for the two-exciton models (Fig. 2) with several intermolecular distances (R). 11-12 + 11-21, 11-22, and 12-22 + 21-22 represent $|\rho^{agg}_{1,1;1,2}(t) + \rho^{agg}_{1,1;2,1}(t)|$, $|\rho^{agg}_{1,1;2,2}(t)|$, and $|\rho^{agg}_{1,2;2,2}(t) + \rho^{agg}_{2,1;2,2}(t)|$, respectively. The unit of optical cycle is $2\pi/m\omega$ [a.u.] (m: division number = 8).

the second quiescent and revival-collapse regions are found to be constructed from a two-photon process: $|\Psi^{agg}_1\rangle - |\Psi^{agg}_2\rangle - |\Psi^{agg}_3\rangle - |\Psi^{agg}_2\rangle - |\Psi^{agg}_1\rangle$. These excitation pathways are schematically shown in Figure 12. It is noted that the split phase distributions are located at $\pm\pi$ for the local maximum amplitude in the first revival-collapse region, while those are located at $\pm 2\pi$ for the local maximum amplitude in the second revival-collapse region.

Conclusions

It is found that the inclusion of a two-exciton state provides a remarkable influence on the relative intensity of the revival-collapse behavior: for the two-exciton model, the first and the second ones originate in the two simultaneous one-photon processes and a two-photon process, respectively; while for the one-exciton model, only a one-photon process exists. For the two-exciton model, since the second excited (two-exciton) state is not so shifted due to the large energy separation between the two-exciton and the ground states, the two-photon process between the ground and the second excited states is expected to be significant. In fact, the second revival-collapse behavior is found to be almost described by the two-photon contribution. For both model systems, the intermolecular-interaction effects are found to shift the first excited state, and then to reduce the one-photon process between the ground and the first excited (one-exciton) states. This reduces the degree of aggregate-photon correlation and then causes the enhancement of revival time, the slow variation in phase properties, and the slow splitting of phase peak. It is also found that the parity of the number of aggregate state model determines the feature of photon-phase splitting and colliding dynamics, which closely relates to the feature of the aggregate-photon correlation dynamics. In relation to this feature, we observe an intermolecular interaction on the dynamical behavior of aggregate-photon correlation described by aggregate entropy S^{agg}. Namely, although the magnitude of S^{agg} in the whole time region becomes small as the intermolecular interaction increases, the momentary variation (decrease) in S^{agg} in the quiescent region of aggregate ground-state population remarkably appears in the intermediate intermolecular interaction case. This feature is found to closely relate to the split behavior of the photon-phase distribution: three split peaks including central standing peak. Since it is already found that the even-numbered state model exhibits no central phase peak [18], the aggregates which provide even-numbered state models (interacting with a coherent field with a relatively large average photon number) are expected to exhibit more remarkable time-dependent variations both in S^{agg} and in off-diagonal aggregate density matrices. In such cases, however, the intermolecular interaction effects are predicted to more rapidly fade out the distinct variation in S^{agg} due to the nonexistence of the

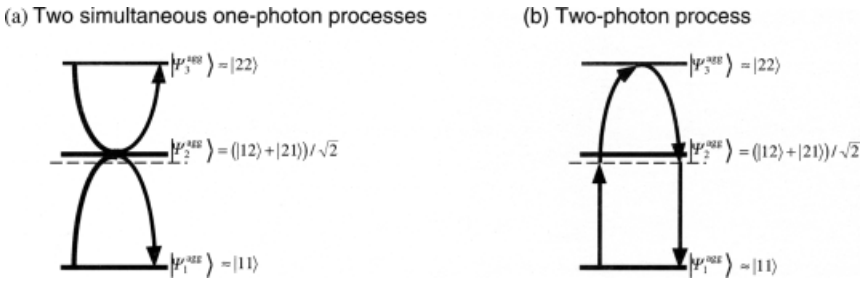

FIGURE 12. Two types of excitation processes [(a) two simultaneous one-photon processes: $|\Psi_3^{agg}\rangle - |\Psi_2^{agg}\rangle - |\Psi_3^{agg}\rangle$ and $|\Psi_1^{agg}\rangle - |\Psi_2^{agg}\rangle - |\Psi_1^{agg}\rangle$, and (b) a two-photon process: $|\Psi_1^{agg}\rangle - |\Psi_2^{agg}\rangle - |\Psi_3^{agg}\rangle - |\Psi_2^{agg}\rangle - |\Psi_1^{agg}\rangle$] for two-exciton dimer models with finite intermolecular distances. The broken line represents the one-exciton state in the noninteracting case. The arrow indicates the excitation pathways.

standing central peak of phase distribution. Judging from the present results and prediction, adjusting the number of aggregates and the intensities of intermolecular interactions is expected to have the possibility of controlling the dynamics of quantum coherency of aggregate and quantized photon field states.

ACKNOWLEDGMENTS

This work was supported by Grant-in-Aid for Scientific Research (No. 10185101, No. 12042248, and No. 12740320) from Ministry of Education, Science, Sports, and Culture of Japan.

References

1. Jaynes, E. T.; Cummings, F. W. Proc IEEE 1963, 51, 100.
2. Allen, L.; Eberly, J. H. Optical Resonance and Two-Level Atoms; Wiley: New York, 1975.
3. Knight, P. L.; Milonni, P. W. Phys Rep 1980, 66, 21.
4. Milonni, P. W.; Singh, S. Advances Atom Molec Opt Phys 1990, 28, 75.
5. Joshi, A.; Lawande, S. V. J Mod Opt 1991, 38, 1407.
6. Filipowicz, P.; Javanainen, J.; Meystre, P. Opt Commun 1986, 58, 327.
7. Parker, J.; Stroud, Jr., C. R.; Phys Rev Lett 1986, 56, 716.
8. Rempe, G.; Walther, H.; Klein, N. Phys Lett 1987, 58, 353.
9. Eberly, J. H.; Narozhny, N. B.; Sanchez-Mondragon, J. J. Phys Rev Lett 1980, 44, 1323.
10. Narozhny, N. B.; Sanchez-Mondragon, J. J.; Eberly, J. H. Phys Rev A 1981, 23, 236.
11. Knight, P. L.; Radmore, P. M. Phys Rev A 1982, 26, 676.
12. Aravind, P. K.; Hirschfelder, J. O. J Phys Chem 1984, 88, 4788.
13. Pegg, D. T.; Barnett, S. M. Europhys Lett 1988, 6, 483.
14. Barnett, S. M.; Pegg, D. T. J Mod Opt 1989, 36, 7.
15. Pegg, D. T.; Barnett, S. M. Phys Rev A 1989, 39, 1665.
16. Eiselt, J.; Risken, H. Phys Rev A 1991, 43, 346.
17. Werner, M. J.; Risken, H. Phys Rev A 1991, 44, 4623.
18. Nakano, M.; Yamaguchi, K. Chem Phys 2000, 252, 115.
19. Nakano, M.; Yamaguchi, K. Chem Phys Lett 1998, 295, 317.
20. Nakano, M.; Yamaguchi, K. Chem Phys Lett 1998, 295, 328.
21. Nakano, M.; Yamaguchi, K. J Phys Chem 1999, 103, 6036.
22. Nakano, M.; Yamaguchi, K. J Chem Phys 2000, 112, 2769.
23. Nakano, M.; Yamaguchi, K. Chem Phys Lett 2000, 317, 103.
24. Nakano, M.; Yamaguchi, K. Chem Phys Lett 2000, 324, 289.
25. Zheng, Z.-M.; Xu, L.; Luo, Z.-F. Phys Rev A 1993, 47, 1557.
26. Peng, J.-s.; Li, G.-x. Phys Rev A 1993, 47, 4212.